In Situ UV–vis–NIR Diffuse Reflectance and Raman Spectroscopic Studies of Propane Oxidation over ZrO$_2$-Supported Vanadium Oxide Catalysts

Xingtao Gao,* Jih-Mirn Jehng,† and Israel E. Wachs*,[1]

**Department of Chemical Engineering, Zettlemoyer Center for Surface Studies, Lehigh University, 7 Asa Drive, Bethlehem, Pennsylvania 18015;
and †Department of Chemical Engineering, National Chung Hsing University, Taichung 402, Republic of China*

The molecular structures and oxidation states of supported 1–5% V$_2$O$_5$/ZrO$_2$ catalysts during propane oxidative dehydrogenation (ODH), with varying propane/O$_2$ ratios, were examined by *in situ* UV–vis–NIR diffuse reflectance and *in situ* Raman spectroscopic studies. The results indicate that the reduction extent of surface V^{5+} cations to V^{3+}/V^{4+} cations under steady-state reaction conditions increases with the propane/O$_2$ ratio. At the same propane/O$_2$ ratio, the relative extent of reduction of the supported V$_2$O$_5$/ZrO$_2$ catalysts generally increases with the surface vanadia loading, and the polymerized surface VO$_4$ species are more extensively reduced than the isolated surface VO$_4$ species during steady-state propane oxidation. The reactivity studies reveal that at the same reaction conditions, both polymerized and isolated surface V cations are active sites for propane oxidation and that the specific catalytic reactivity (as measured by turnover frequency; TOF) is independent of the surface density of the two-dimensional vanadia overlayer on the ZrO$_2$ support. Furthermore, the relatively constant TOF with surface vanadia coverage demonstrates that propane ODH to propylene requires only one surface VO$_4$ site. However, the propylene selectivity increases with increasing surface vanadia loading due to the removal of nonselective surface sites, possibly terminal Zr–OH groups, on the ZrO$_2$ surface by the deposition of surface vanadia species. The propane/O$_2$ ratio greatly affects the selectivity of these catalysts. Highly oxygen-rich environments (e.g., propane/O$_2$ ratio = 1/10) give rise to the highest propylene selectivity, revealing that propylene production is favored on highly oxidized surface vanadia (+5) sites. Small V$_2$O$_5$ crystallites above monolayer surface vanadia coverage do not contribute to propane ODH because of their low dispersion and low number of active surface sites (spectator vanadia species). © 2002 Elsevier Science (USA)

Key Words: catalysts; supported vanadium oxide; V$_2$O$_5$/ZrO$_2$; propane oxidative dehydrogenation; *in situ* characterization; Raman, UV–vis–NIR diffuse reflectance spectroscopy.

INTRODUCTION

Vanadium oxide is a well-established catalyst for partial oxidation of lower alkanes (1). It has been widely employed as an active component in bulk mixed metal oxides and supported vanadia catalysts for oxidative dehydrogenation (ODH) of propane. It was found that the oxide supports and promoters significantly affect the selectivity and activity of supported vanadia species for propane ODH through modification of the redox and acid–base properties of the catalysts (2–6). Khodakov *et al.* (7, 8), however, concluded that the turnover frequencies (TOFs) do not directly depend on the identity of the oxide support but on the domain size of the surface VO$_x$ species and that intermediate surface VO$_x$ domain sizes provide a maximum activity. The low propane ODH selectivity toward propene for low surface vanadia density and bulk ZrV$_2$O$_7$ was attributed to exposed nonselective V–O–Zr and Zr–O–Zr sites. However, a later study of the VO$_x$/ZrO$_2$ system by the same group, employing a different preparation method, showed that bulk ZrV$_2$O$_7$ is quite selective (9). This suggests that some other factors, rather than V–O–Zr sites since ZrV$_2$O$_7$ is exclusively composed of V–O–Zr functionalities, contribute to total combustion during propane ODH.

Kinetic isotopic studies of propane ODH over V$_2$O$_5$/ZrO$_2$ catalysts by Chen *et al.* (10–12) suggested that both the dissociative O$_2$ chemisorption and the rate-determining C–H bond activation steps are irreversible. Their results further confirm a Mars–van Krevelen type redox mechanism for propane ODH over supported vanadia catalysts. However, all of these studies (7–12) were conducted under propane-rich reaction environments (propane/oxygen ≫ 1).

The influence of the propane/oxygen ratio over a wide range on the reduction extent of surface V cations (percentage of V^{4+}/V^{3+} during steady-state reaction) and the possible effect of reduction extent on the reactivity and selectivity of supported vanadia catalysts during propane ODH have not yet been examined in the literature. The degree of reduction of the oxide catalysts during redox cycle, which has been associated with the increase of the binding strength of surface lattice oxygen, was proposed to be the major factor in determining the reaction rates of

butane oxidation and the selectivities to partial oxidation products (13). However, *in situ* UV–vis diffuse reflectance spectroscopy (DRS) studies during *n*-butane oxidation to maleic anhydride do not reveal any relationship among extent of reduction, TOF, and selectivity (14). In addition, the catalytic behaviors of the isolated and polymerized surface vanadia species for alkane oxidation are still under discussion in the literature (7, 15, 16). For propane oxidative dehydrogenation over V_2O_5/Al_2O_3 catalysts, the same selectivity vs conversion curves are obtained and the catalytic activity, if converted to TOF values from the literature results, is only slightly higher at high surface vanadia loadings (less than 2 times) (15). In contrast, other studies conclude that the polymerized surface vanadia species on the oxide supports are more selective and active than the isolated surface vanadia species for propane ODH (7). Thus, the *in situ* measurements of the structure and oxidation states of the active surface vanadium oxide species is of key importance for a more detailed fundamental understanding of the relationships between the catalytic performance and the redox ability and the molecular structure of the active surface vanadia species.

Previous *in situ* UV–vis–NIR DRS studies (16) of supported vanadia catalysts during ethane and *n*-butane oxidation have shown that only a small fraction of surface V(V) sites are reduced to V(IV)/V(III) cations under oxygen-rich steady-state reaction conditions and the extents of reduction of the surface V(V) species is a strong function of the specific oxide support: $V_2O_5/ZrO_2 > V_2O_5/Al_2O_3 > V_2O_5/SiO_2$. It was also found that the alumina- and silica-supported vanadia catalysts exhibit very limited reduction during C_2 and C_4 alkane ODH and oxidation, respectively. The present work focuses on the extent of reduction, molecular structure, and oxidation state changes of supported V_2O_5/ZrO_2 catalysts during propane ODH (using an improved UV–vis Harrick cell since the errors introduced through inaccurate sample temperature readings for the commercial Harrick cell were found to be generally more than $100°C$). The results obtained should enable the establishment of the fundamental relationships between the extent of reduction of the surface V sites, ratio of V(V) to V(VI)/V(III), during propane ODH and the reactivity and selectivity of the catalysts.

EXPERIMENTAL

Catalyst preparation. The support used for this study was ZrO_2 (Degussa, $S_{BET} = 34 \, m^2/g$) which possesses a well-crystallized monoclinic structure. The 1–5% V_2O_5/ZrO_2 samples were prepared by the incipient-wetness impregnation of isopropanol solutions of vanadium isopropoxide ($VO(O–Pr^i)_3$, Alfa-Aesar 97% purity) on the ZrO_2 support. The preparation was performed inside a glove box

with continuously flowing N_2. After impregnation, the samples were kept inside the glove box overnight. The samples were subsequently dried in flowing N_2 at $120°C$ for 1 h and at $300°C$ for another hour and were finally calcined in flowing air at $300°C$ for 1 h and $450°C$ for 2 h. The 4% V_2O_5/ZrO_2 sample possesses a monolayer coverage of the surface vanadia species with a surface density of 8.1V atoms/nm^2 (17).

UV–vis–NIR DRS. The DRS experiments were performed on a Varian Cary 5E UV–vis–NIR spectrophotometer. Two types of reflectance cells were employed, an *in situ* Harrick cell and a quartz flow cell, which have been described in detail elsewhere (18). The quartz cell combined with the integration sphere Praying Mantis Diffuse Reflectance Attachment (DRA) was used for the H_2-reduced samples as references. The reference DRS spectra of the reduced samples were recorded in the region of 200–2200 nm at room temperature. A halon white (PTFE) reflectance standard was used as the baseline. The spectra of the dehydrated supported V_2O_5/ZrO_2 samples were obtained after the samples were calcined at $500°C$ in flowing O_2/He for 1 h. The spectra of the reduced samples were taken after the dehydrated supported V_2O_5/ZrO_2 samples were reduced at $500°C$ for 1 h in 10% H_2/Ar (Scott Specialty Gases, Inc.) with a flow rate of 30 mL/min.

In situ DRS spectra were taken in the range of 200–800 nm using a Harrick DRS cell (HVC-DR2) with DRA to perform the measurements under reaction conditions at high temperatures. The Harrick cell was slightly modified to accurately measure the temperature around the surface of the sample powder. A second thermocouple was added to the sample cup with the probe tip just under the sample surface and close to the spot for spectral recording that is usually around the center of the sample cup. This thermocouple line should not touch the sample cup, which usually possesses a higher temperature than the sample. The Cu sample cup (which has excellent thermal conductivity but poor heat capacity) usually heats up very quickly, while the temperature of the sample increases relatively slowly. After the sample temperature was stabilized, this temperature was found to be much lower than the set-point temperature of the sample cup shown on the temperature controller. This fact is in agreement with the previous finding by Venter and Vannice (19) for an older type Harrick DRIFTS cell (HVC-DRP). Table 1 lists the temperature differences under various conditions. It is also noted that the higher the set-point temperature, the larger the difference in temperature. The surface temperature of a sample seems also to be a function of gas composition, and the heat generated by the exothermic propane ODH reaction tends to decrease the temperature difference.

All samples for the *in situ* measurements were first calcined in the oven at $450°C$ for 1 h before immediate transfer

<div style="text-align:center">

TABLE 1

Temperature Differences between Harrick Cell (HVC-DR2) Sample Cup and the Catalyst Surface for Different Gas Compositions at 300°C

</div>

Gas mixture	ΔT_1 at 300 (°C)^a		
	1% V$_2$O$_5$/ZrO$_2$	2% V$_2$O$_5$/ZrO$_2$	4% V$_2$O$_5$/ZrO$_2$
20% O$_2$/He	125	123	120
1.6% C$_3$/8% O$_2$/He	121	119	116
18% C$_3$/18% O$_2$/He	106	96	95
18% C$_3$/3% O$_2$/He	106	102	100
18% C$_3$/He	109	106	104

^{a} ΔT_1 (°C) = T (set-point) − 300°C (sample).

to the *in situ* cell. The sample in the cell was then pretreated at a sample surface temperature of 400°C (or 570–580°C at the sample cup) in O$_2$/He for 1 h before any further treatment. The dehydrated ZrO$_2$ support at the corresponding reaction temperature was used as the baseline reference for the supported V$_2$O$_5$/ZrO$_2$ catalysts. Propane oxidation with varying C$_3$H$_8$/O$_2$ ratios (1 : 5 = 0.8C$_3$H$_8$/4O$_2$/45.2He; 1 : 1 = 9C$_3$H$_8$/9O$_2$/32He, and 6 : 1 = 9C$_3$H$_8$/1.5O$_2$/39.5He) and propane reduction (9C$_3$H$_8$/41He) were performed at different temperatures with a total flow rate of 50 cm^3/min.

The DRS spectra were processed with the Bio-Rad Win-IR software, consisting of calculation of the Kubelka–Munk function ($F(R_\infty)$) from the absorbance. The edge energy (E_g) for allowed transitions was determined by finding the intercept of the straight line in the low energy rise of a plot of $(F(R_\infty) \times h\nu)^2$ against $h\nu$, where $h\nu$ is the incident photon energy (20).

In situ Raman spectroscopy. The *in situ* Raman spectrometer system consists of a quartz cell with a sample holder, a triple-grating spectrometer (Spex, Model 1877), a CCD detector (Jobin Yvon-Spex, ISA Inc., Model Spectrum-1), and an argon ion laser (Spectra-Physics, Model 165). The sample holder is made from a metal alloy (Hastalloy C), and a 100- to 200-mg sample disk is held by the cap of the sample holder. The sample holder is mounted onto a ceramic shaft which is rotated by a 115 V DC motor at a speed of 1000–2000 rpm. A cylindrical heating coil surrounding the quartz cell is used to heat the cell. The quartz cell is capable of operating up to 600°C and flowing gas is introduced into the cell at a rate of 50–100 cm^3/min at atmospheric pressure.

The *in situ* Raman spectra were obtained along the following procedures. The sample was placed into the cell and initially heated to 500°C for 1 h in a flow of ∼20% O$_2$ balanced with He gas (Scott Specialty Gases, Inc.). The dehydrated Raman spectrum was collected after cooling the sample to 300°C in a flow of O$_2$/He gas for 30 min. Then, a C$_3$H$_8$/He (Scott Specially Gases, Inc.) and O$_2$/He gaseous

mixture with varying C$_3$H$_8$/O$_2$ ratios (1 : 5 = 1.6C$_3$H$_8$/8O$_2$/ 30.4He; 1 : 1 = 9C$_3$H$_8$/9O$_2$/32He; 3 : 1 = 9C$_3$H$_8$/3O$_2$/38He; 9 : 1 = 9C$_3$H$_8$/1O$_2$/40He) was introduced into the cell and the Raman spectrum during propane oxidation at 300°C was collected after reaching steady state. Finally, after the propane oxidation reaction the sample was reoxidized from 300 to 500°C under flowing O$_2$/He gas.

Propane oxidation. Propane oxidation was carried out in an isothermal fixed-bed differential reactor (Pyrex tubing, 1/4″OD and 1 ft long) using 20–100 mg of catalyst at atmospheric pressure. The reactant gas mixtures of C$_3$H$_8$/ O$_2$ in He with varying flow ratios of 1 : 10 = 0.5C$_3$H$_8$/ 5O$_2$/44He, 1 : 2 = 4.5C$_3$H$_8$/9O$_2$/32He, and 3 : 1 = 4.5C$_3$H$_8$/ 1.5O$_2$/39.5He (cm^3/min) were used. The reactor effluent was analyzed by an on-line Hewlett–Packard Gas Chromatograph 6890 Series equipped with both TCD and FID detectors. A Carboxene-1000 packed column and a Supelco capillary column (column No. PQ1334-04) were employed in parallel for TCD and FID, respectively. The samples were pretreated in a stream of O$_2$/He gas mixture at 450°C for 0.5 h before each run. The activity values, as measured by turnover frequency (the number of propane molecules converted per V atom per second), were obtained at reaction temperatures of 300 and 350°C.

RESULTS AND DISCUSSION

The *in situ* UV–vis DRS spectra of 4% V$_2$O$_5$/ZrO$_2$ at 300°C under various gas compositions are shown in Fig. 1. The oxygen ligand to metal charge transfer (LMCT) bands of V(V), located above 20,000 cm^{-1}, decrease as the propane/O$_2$ ratio increases, indicating an increase in the reduction of surface V(V) cations. Simultaneously, weak d–d
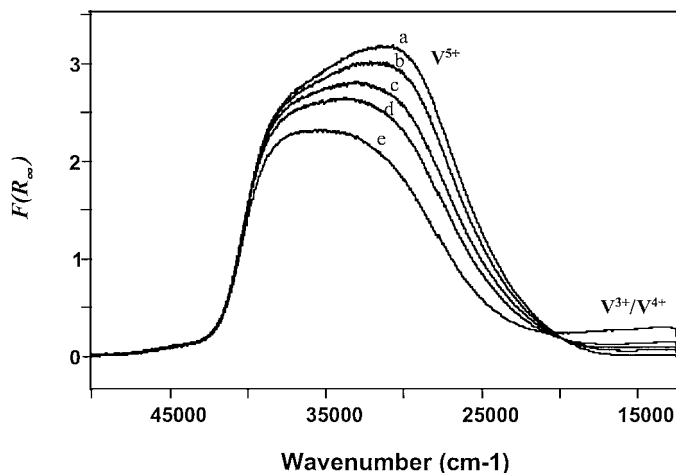

FIG. 1. *In situ* UV–vis spectra of 4% V$_2$O$_5$/ZrO$_2$ at 300°C in (a) O$_2$/He; (b) 1 : 5 = 0.8C$_3$H$_8$/4O$_2$/45.2He; (c) 1 : 1 = 9C$_3$/9O$_2$/32He; (d) 6 : 1 = 9C$_3$H$_8$/1.5O$_2$/39.5He; and (e) 9C$_3$H$_8$/41He (cm^3/min).

Relative Extents of Reduction of the Supported V_2O_5/ZrO_2 Catalysts at Different Gas Compositions at 300°C

Catalyst	1:5 C_3H_8/O_2 (%)	1:1 C_3H_8/O_2 (%)	6:1 C_3H_8/O_2 (%)	18% $C_3/H_8/He$ (%)
1% V_2O_5/ZrO_2	1.8	4.6	4.9	12.9
2% V_2O_5/ZrO_2	1.6	5.5	7.8	19.8
4% V_2O_5/ZrO_2	8.2	19.6	29.9	50.8

Note. Total flow rate = 50 ml/min. The C_3H_8/O_2 ratios are 1:5 = 1.6% C_3H_8/8% O_2; 1:1 = 18% C_3/18% O_2, and 6:1 = 18% C_3H_8/3% O_2 with balance of He. The relative decrease of the LMCT band area = $(1 - A_{rxn}/A_0')/(1 - A_{red}/A_0)$, where A_0 or A_0' is the LMCT band area of the corresponding oxidized catalyst before reduction or reaction, respectively, A_{red} is the area of the H_2-reduced reference catalyst, and A_{rxn} is the area of the catalyst during alkane oxidation/reduction.

transition bands of V(IV)/V(III) cations, located below 20,000 cm^{-1}, increase with the propane/O_2 ratio. By using the method developed previously in Ref. 16, the relative extents of reduction of the 1, 2 and 4% V_2O_5/ZrO_2 catalysts during propane oxidation at different gas compositions were obtained, as shown in Table 2. The corresponding edge energy shifts are listed in Table 3. At the same propane/O_2 ratio, the relative extent of reduction of the V_2O_5/ZrO_2 catalysts generally increases with the surface vanadia loading. The 1 and 2% V_2O_5/ZrO_2 catalysts, with mostly isolated surface VO_4 species, do not exhibit a significant edge energy shift with varying propane/O_2 ratios. The edge energy of the 4% V_2O_5/ZrO_2 catalyst, with a high concentration of polymerized surfaceVO_4 species (17), increases with increasing propane/O_2 ratio, indicating that polymerized surface VO_4 species are more easily reduced in reducing environments. The easier reduction of polymerized surface VO_4 species suggests higher availability of bridging oxygen in V–O–V bonds than oxygen in the isolated surface VO_4 species.

The *in situ* Raman spectra of the 5% V_2O_5/ZrO_2 sample (~1.25 monolayers) during the propane oxidation reaction at 300°C are presented in Fig. 2. The initial dehydrated Raman spectrum (Fig. 2a) indicates that supported vandium oxide is present as both surface vanadia species and small V_2O_5 crystallites (major Raman bands at ~994, ~700, ~402, ~280, and ~146 cm^{-1}). The Raman band at

Edge Energy Shifts of the Supported V_2O_5/ZrO_2 Catalysts at Different Gas Compositions at 300°C

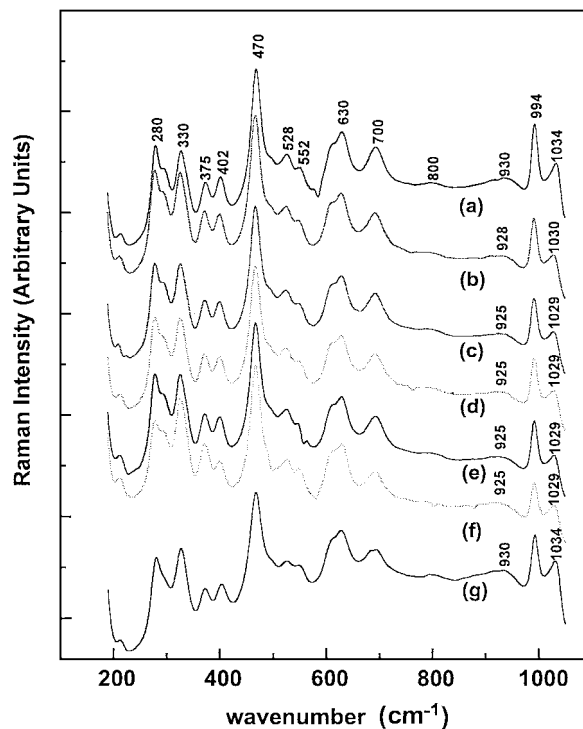| Catalyst	E_g (eV)				
	O_2/He	1:5 C_3/O_2	1:1 C_3/O_2	6:1 C_3/O_2	C_3H_8/He
1% V_2O_5/ZrO_2	3.40	3.34	3.33	3.33	3.33
2% V_2O_5/ZrO_2	3.29	3.25	3.25	3.27	3.32
4% V_2O_5/ZrO_2	3.14	3.17	3.20	3.24	3.30

FIG. 2. *In situ* Raman spectra of 5% V_2O_5/ZrO_2 at 300°C in (a) 20% O_2/He; (b) 1:5 = 1.6C_3H_8/8O_2/30.4He; (c) 1:1 = 9C_3/9O_2/32He; (d) 3:1 = 9C_3H_8/3O_2/38He; (e) 9:1 = 9C_3H_8/1O_2/40He; and (f) 9C_3H_8/41He (cm^3/min); and in (g) 20% O_2/He at 500°C.

~1034 cm^{-1} is characteristic of the dehydrated surface vanadate species possessing one terminal V=O bond and three bridging V–O–M bonds, where M is either a Zr support cation or another surface V atom (21–27), and the broad Raman band at ~935 cm^{-1} is characteristic of the bridging V–O–V bond of the dehydrated polymeric surface vanadate species (21, 24, 27–29). Furthermore, the polymeric surface vanadate species also possess a terminal V=O bond at ~1020 cm^{-1} which overlaps with the Raman band of the isolated surface vanadate species (30). This is consistent with the Khodakov *et al.* (7, 8) studies on supported vanadium oxide catalysts that conclude that both surface polyvanadate and monovanadate species coexist on the ZrO_2 support. Thus, this sample contains ~4% V_2O_5 as surface vanadia species and ~1% V_2O_5 as small V_2O_5 crystallites. The Raman scattering cross section of V_2O_5 crystallites is ~10 times greater than that of the surface vanadia species (31). The Raman features of the ZrO_2 support (Raman bands at ~630, ~552, ~528, ~470, ~375, and ~330 cm^{-1}) agree with the monoclinic phase of ZrO_2.

During propane ODH at 300°C, the isolated and polymeric surface vanadate species as well as the small V_2O_5 crystallites are partially reduced under the reaction conditions (reflected by the decrease of the *in situ* Raman intensities; see Figs. 2b–2f). The extent of reduction of the surface vanadia species increases with increasing C_3H_8/O_2
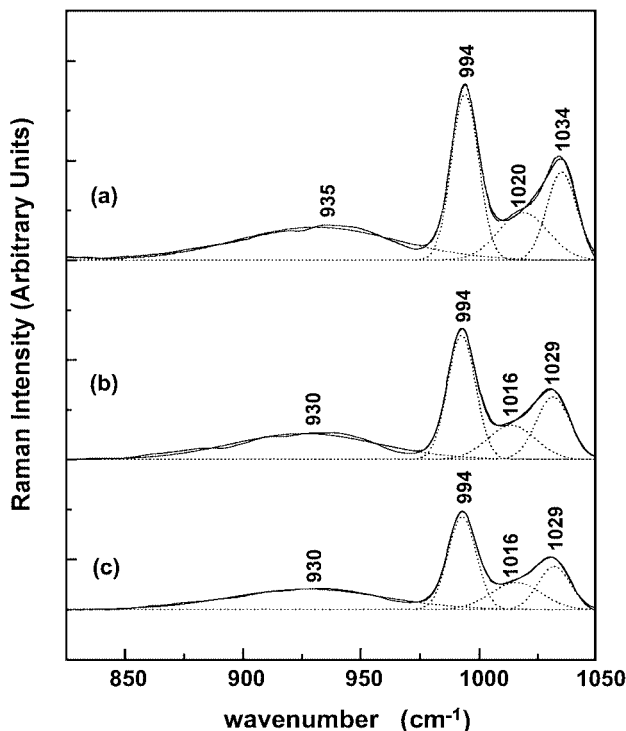
FIG. 3. A multiple Gaussian fitting on *in situ* Raman spectra of the 5% V$_2$O$_5$/ZrO$_2$ catalyst in the 800–1100 cm^{-1} region at 300°C in (a) 20% O$_2$/He; (b) 1 : 5 = 1.6C$_3$H$_8$/8O$_2$/30.4He; and (c) 9 : 1 = 9C$_3$H$_8$/1O$_2$/40He.

ratio in the feed, and the reduced surface vanadia species can be restored to its original oxidized form upon reoxidation (Fig. 2g). This is consistent with the *in situ* UV–vis–NIR DRS results in Table 2 that the amount of reduced surface vanadia species increases with increasing C$_3$H$_8$/O$_2$ ratio. In Fig. 2, the *in situ* Raman spectra under different environments cannot clearly distinguish the reduction between the surface isolated and polymeric vanadate species as a result of their broad Raman bands in the V$_2$O$_5$/ZrO$_2$ catalyst. Consequently, a multiple Gaussian equation was applied to fit the *in situ* Raman spectra in the 800–1050 cm^{-1} region as a function of C$_3$H$_8$/O$_2$ ratio. The results are shown in Fig. 3 by assuming four Raman peaks with corresponding surface vanadate structures and small V$_2$O$_5$ crystallites appear in the 1010–1035 cm^{-1} region. Raman peak intensities are normalized with the strongest Raman peak at ~470 cm^{-1} of the ZrO$_2$ support. A quantitative analysis of the decrease of the peak area suggests that the reduction of the isolated surface vanadate species (Raman peak at ~1034 cm^{-1}) is calculated to be 19% with increasing C$_3$H$_8$/O$_2$ ratio from 0 to 0.2 and to be 35% with increasing C$_3$H$_8$/O$_2$ ratio from 0 to 9. The reduction of the Raman intensities at ~1020 and ~935 cm^{-1} (characteristic of the terminal V=O and bridging V–O–V of the polymeric surface vanadate species) are calculated to be 31 and 29%, respectively, upon increasing the C$_3$H$_8$/O$_2$ ratio from 0 to

0.2, and 43 and 40%, upon increasing the C$_3$H$_8$/O$_2$ ratio from 0 to 9, respectively. The reduction of small V$_2$O$_5$ crystallites (Raman intensity at ~994 cm^{-1}) is determined to be 23% upon increasing the C$_3$H$_8$/O$_2$ ratio from 0 to 0.2 and 36% upon increasing the C$_3$H$_8$/O$_2$ ratio from 0 to 9. These calculations confirm that the polymeric surface vanadate species are more extensively reduced than the isolated surface vanadate species under steady-state reaction conditions and that the extent of reduction of the V$_2$O$_5$/ZrO$_5$ catalysts increases with increasing C$_3$H$_8$/O$_2$ ratio.

The catalytic results of propane oxidation over the V$_2$O$_5$/ZrO$_2$ catalysts are presented in Table 4. Pure ZrO$_2$ produces predominantly CO$_x$ products and the CO$_x$ selectivity decreases with increasing surface vanadia coverage. It is apparent from Table 4 that at the same propane/O$_2$ ratio, the propylene selectivity at a similar propane conversion increases with surface vanadia coverage. The monolayer 4% V$_2$O$_5$/ZrO$_2$ sample exhibits the highest propylene selectivity, especially at low propane conversions. The decrease of CO$_x$ production with increasing surface vanadia coverage may be associated with the removal of nonselective surface sites on the ZrO$_2$ support by the deposition of the surface vanadia species. As shown in Fig. 4, pure ZrO$_2$ exhibits two bands at 7392 and 7194 cm^{-1}, which are assigned to the overtone vibrations of terminal and bridging hydroxyls on the zirconia surface (32). The intensity of the terminal Zr–OH band at 7392 cm^{-1} significantly decreases with increasing surface vanadia coverage. It was found that the terminal Zr–OH hydroxyls are more reactive than the bridging hydroxyls and can exchange hydrogen from propylene more rapidly (32). Thus, the production of CO$_x$ on ZrO$_2$ may be associated with the presence of exposed Zr–OH hydroxyls, which may facilitate the formation of intermediates of radical C$_3$H$_7$ and/or O$_2^-$ ions for the formation of CO$_x$, as observed by *in situ* IR spectroscopy (33). The deposition of
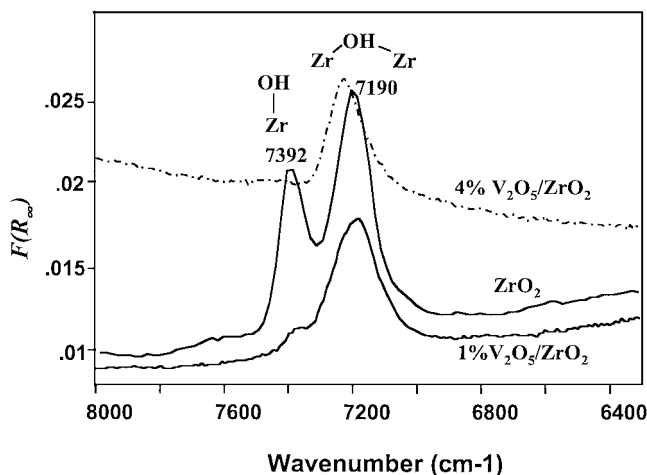

FIG. 4. NIR DRS spectra of the dehydrated supported V$_2$O$_5$/ZrO$_2$ samples.

TABLE 4

Catalytic Results of Propane Oxidation over the Supported V_2O_5/ZrO_2 Catalysts at 300 and 350°C ($1:10 = 0.5C_3H_8/5O_2/44$ He; $1:2 = 4.5C_3H_8/9O_2/32$He, and $3:1 = 4.5C_3H_8/1.5O_2/39.5$He ($cm^3$/min))

Catalyst	Reaction T (°C)	C_3H_8/O_2	Conv.	$A_c{}^a$ (mmol/g·h)	TOF^b ($10^{-3} S^{-1}$)	Selectivity[c]			
						C_3H_6	CO	CO_2	C_3H_4O
ZrO_2	350	1:10	1.2	0.1		16.0	41.6	42.4	0
		1:2	0.6	0.3		1.9	48.5	49.6	0
		3:1	0.2	0.1		13.7	46.2	40.1	0
1% V_2O_5/ZrO_2	300	1:10	2.4	0.3	0.8	50.4	24.6	25.0	0
		1:2	1.6	1.8	4.4	35.2	24.2	40.5	0.1
		3:1	0.9	1.0	2.5	50.6	19.5	29.9	tr
	350	1:10	6.8	0.9	2.3	43.5	29.5	27.0	0
		1:2	9.3	10.2	51.5	31.6	31.4	36.9	0.1
		3:1	3.4	3.7	9.4	45.1	27.4	27.5	tr
2% V_2O_5/ZrO_2	300	1:10	2.0	0.8	1.0	73.2	14.6	12.2	0
		1:2	1.0	3.1	4.0	63.3	19.4	17.3	tr
		3:1	0.7	2.2	2.8	67.2	17.9	14.9	tr
	350	1:10	5.7	2.2	2.8	59.6	24.3	16.1	0
		1:2	4.5	14.2	18.0	47.9	30.1	22.0	tr
		3:1	2.5	7.9	10.0	56.6	25.5	17.9	tr
4% V_2O_5/ZrO_2	300	1:10	2.0	1.0	0.6	80.0	14.0	6.0	tr
		1:2	1.0	3.9	2.4	74.5	18.0	7.3	0.2
		3:1	0.7	2.7	1.7	77.8	16.0	6.1	0.1
	350	1:10	5.2	2.4	1.6	62.1	28.7	9.1	0.1
		1:2	3.6	14.0	8.8	53.5	34.8	11.3	0.4
		3:1	2.8	10.9	6.9	58.5	31.2	9.9	0.4

[a] Millimoles of propane converted per gram catalyst per hour.
[b] TOF is calculated on the basis of the total V atoms in the catalysts for propane conversion.
[c] tr = trace.

surface vanadia species consumes mostly the terminal Zr–OH surface hydroxyls, resulting in a significant decrease in the formation of CO_x. Thus, the surface vanadia coverage effect on the propylene selectivity is most probably related to the removal of nonselective sites on the ZrO_2 surface rather than to structural difference between isolated and polymerized surface vanadia species at different surface vanadia coverages.

In addition, the propane/O_2 ratio significantly affects the propylene selectivity. The selectivity vs conversion at different propane/O_2 ratios over the 4% V_2O_5/ZrO_2 sample is presented in Fig. 5. The high oxygen concentration at a propane/O_2 ratio of 1/10 gives rise to the highest propylene selectivity. Similar results were also obtained for the catalysts possessing lower surface vanadia coverages. This strongly suggests that propylene production is favored on highly oxidized surface vanadia species of the V_2O_5/ZrO_2 catalyst where the surface V^{5+} population is over 90%. This may be related to the propene and CO_x formation mechanisms where surface V^{5+} is the active site for propene formation and reduced surface V^{4+}/V^{3+} sites favor CO_x formation via an oxygenated intermediate (34).

Interestingly, a very small amount of the oxygenated product (CH_2CHCHO) is observed at propane/O_2 ratios of 1/2

and 3/1, and the monolayer catalyst shows a selectivity of 0.4%. More recent studies further reveal that for supported V_2O_5/Nb_2O_5 catalysts significant amounts of acrolein are obtained under high C_3H_8/O_2 ratios (35). The relatively rich
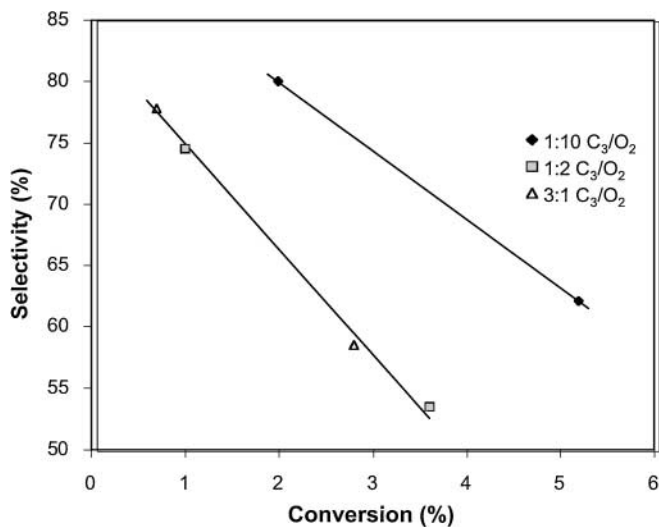

FIG. 5. Propylene selectivity vs conversions obtained at 300 and 350°C at different propane/O_2 ratios for supported 4% V_2O_5/ZrO_2 catalysts.
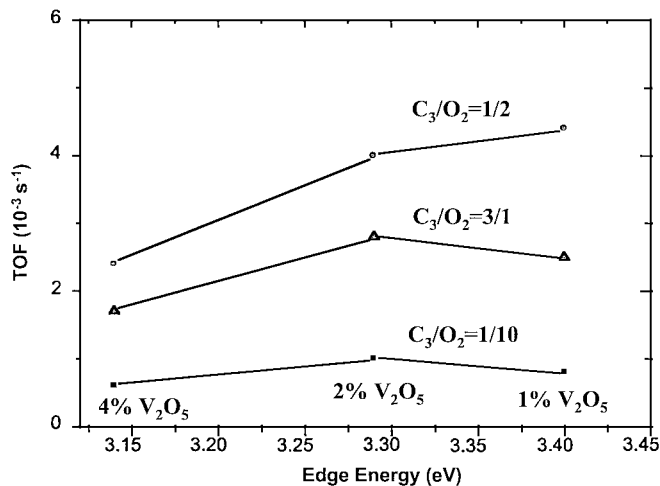
FIG. 6. The specific catalytic activity (TOF) vs *in situ* edge energy of supported V$_2$O$_5$/ZrO$_2$ catalysts during propane oxidation at various propane/O$_2$ ratios.

propane stream gives rise to a more reduced surface that favors the formation of oxygenates (e.g., acrolein). This is probably due to activation of the methylene group of propylene to form surface allyl intermediates on the reduced surface vanadia sites and the oxygen insertion on a adjacent surface V (+5) site (34). For supported V$_2$O$_5$/Nb$_2$O$_5$ catalysts, the small V$_2$O$_5$ crystallites slightly above monolayer coverage have been found to have no effect on the propane ODH and proplyene selectivity. However, extremely high contents of V$_2$O$_5$ crystallites have a negative effect on the propane ODH reaction because they are not intrinsically as active (low dispersion) and cover the active surface vanadia sites (35).

The specific catalytic activity, TOF, as a function of the *in situ* dehydrated edge energy during propane oxidation at various propane/O$_2$ ratios is presented in Fig. 6. The high edge energy of 3.40 eV corresponds to isolated surface VO$_4$ species in the dehydrated 1% V$_2$O$_5$/ZrO$_2$ sample, while the low edge energy of 3.14 eV corresponds to the coexistence of polymerized surface VO$_4$ species in the dehydrated V$_2$O$_5$/ZrO$_2$ sample (17). The propane/O$_2$ ratio appears to have a significant effect on the TOF values of these catalysts. The relatively high activity at propane/O$_2$ ratio of 1/2 (9% C$_3$H$_8$/18% O$_2$) may be due to its relatively high oxygen and propane concentrations. However, no significant variation in the specific catalytic activity, TOF, is observed for these catalysts under the same reaction conditions, which indicates that both isolated and polymerized V sites are active sites and that the edge energy/domain size of the surface vanadia species has only a minor effect on the activity of the supported V$_2$O$_5$/ZrO$_2$ catalysts. The relatively constant TOF values as a function of surface vanadia species support the conclusion that only one surface V site is needed for propane ODH to propylene, in agreement with the conclusion by Eon *et al.* (15) at CNRS-Lyon, France. The

constant TOF values as a function of surface vanadia coverage for propane oxidation has also been observed for the suported V$_2$O$_5$/Nb$_2$O$_5$ system by Watling *et al.* at University of Twente, the Netherlands (36), and has recently been confirmed by Zhao and Wachs at Lehigh University (35). However, Khodakov *et al.* (7, 8) found that the turnover frequencies increase with the surface vanadia coverage on different oxide supports. Specifically, it is the domain size of the surface vanadia species and the intermediate surface vanadia domain sizes that control catalytic activity. The origin of the difference between the present finding and that of Khodakov is not well understood at the present time (37). Some differences in the sample preparation can be considered. The ZrO$_2$ support employed in the present study is a commercial product possessing the tetragonal phase, while Kodakov *et al.* employed zirconium oxyhydroxide as the initial support, which is homemade from the precipitation of zirconyl chloride. The zirconium oxyhydroxide support possesses a high surface concentration of hydroxyl groups and surface area. Furthermore, both monoclinic and tetragonal phases were observed for the Berkeley catalysts, depending on the calcination temperature and the vanadia loading. It is suspected that possible chloride residue from the ZrO$_2$ support precursor, the different ZrO$_2$ phases, higher surface hydroxyl density, or the V–Zr–O$_x$ solid solution, which has been shown to be present in the V$_2$O$_5$/ZrO$_2$ catalysts prepared by a similar method (38), may partially contribute to the above differences.

CONCLUSIONS

In situ UV–vis–NIR DRS and Raman spectroscopic studies of supported V$_2$O$_5$/ZrO$_2$ catalysts during propane oxidation indicate that varying amounts of surface V(V) sites are reduced to V(IV)/V(III) cations under steady-state reaction conditions, depending on the propane/O$_2$ ratio, reaction temperature, and surface vanadia loading. The polymerized surface vanadia species are generally more extensively reduced than the isolated surface vanadia species during steady-state propane oxidation. The catalytic results demonstrate that the surface density of the two-dimensional surface vanadia overlayer does not significantly affect the reactivity (TOF) of the catalysts and that both polymerized and isolated surface vanadia species appear to be the active sites for propane ODH reaction. The relatively constant TOF with surface vanadia coverage demonstrates that propane ODH to propylene requires only one surface vanadia site. The propylene selectivity is a function of surface vanadia loading, which is believed to be associated with the removal of the nonselective sites, isolated Zr–OH, by the deposition of surface vanadia species. The surface vanadia species oxidation state, which is a function of propane/O$_2$ ratio and vanadia loading, greatly affects the selectivity of the catalysts. Highly

oxygen-rich environments (e.g., propane/O_2 ratio $= 1/10$) give rise to the highest propylene selectivity, suggesting that propylene production is favored on highly oxidized surface vanadia species present in supported V_2O_5/ZrO_2. Highly reducing environments (e.g., propane/$O_2 = 9/1$) form small amounts of acrolein, which are thought to be related to activation of the methylene C–H bonds of propylene on the reduced surface vanadia sites. The small V_2O_5 crystallites above monolayer coverage are essentially spectator vanadia species during propane ODH to propylene since their low dispersion and low number of active surface sites prevent them from making any significant contribution.

ACKNOWLEDGMENTS

REFERENCES

1. Mamedov, E. A., and Corberan, V. C., *Appl. Catal. A* **127**, 1 (1995).
2. Lemonidou, A. A., Nalbandian, L., and Vasalos, I. A., *Catal. Today* **61**, 333 (2000).
3. Arena, F., Frusteri, F., and Parmaliana, *Catal. Lett.* **60**, 59 (1999).
4. Ermini, V., Finocchio, E., Sechi, S., Busca, G., and Rossini, S., *Appl. Catal. A* **198**, 67 (2000).
5. Lopez Nieto, J. M., Coenraads, R., Dejoz, A., and Vazquez, M. I., *Stud. Surf. Sci. Catal.* **110**, 443 (1997).
6. Al-Zahrani, S. M., Jibril, B. Y., and Abasaeed, A. E., *Ind. Eng. Chem. Res.* **39**, 4070 (2000).
7. Khodakov, A., Olthof, B., Bell, A. T., and Iglesia, E., *J. Catal.* **181**, 205 (1999).
8. Khodakov, A., Yang, J., Su, S., Iglesia, E., and Bell, A. T., *J. Catal.* **177**, 343 (1998).
9. Male, J. L., Niessen, H. G., Bell, A. T., and Tilley, T. D., *J. Catal.* **194**, 431 (2000).
10. Chen, K., Khodakov, A., Yang, J., Bell, A. T., and Iglesia, E., *J. Catal.* **186**, 325 (2000).
11. Chen, K., Xie, S., Iglesia, E., and Bell, A. T., *J. Catal.* **192**, 197 (2000).
12. Chen, K., Bell, A. T., and Iglesia, E., *J. Phys. Chem. B* **104**, 1292 (2000).
13. Andersen, P. J., and Kung, H. H., *in* "Proceedings of the 10th International Congress on Catalysis, Budapest, 1992" (L. Guczi, F. Solymosi, and P. Tetenyi, Eds.), p. 205. Akadémiai Kiadò, Budapest, 1993.
14. Wachs, I. E., Jehng, J. M., Deo, G., Weckhuysen, B. M., Guliants, V. V., Bensiger, J. B., and Sundaresan, S., *J. Catal.* **170**, 75 (1997).
15. Eon, J. G., Olier, R., and Volta, J. C., *J. Catal.* **145**, 318 (1994).
16. Gao, X., Banares, M. A., and Wachs, I. E., *J. Catal.* **188**, 325 (1999).
17. Gao, X., and Wachs, I. E., *J. Phys. Chem.* **104**, 1261 (2000).
18. Weckhuysen, B. M., and Schoonheydt, R. A., *Catal. Today* **49**, 441 (1999).
19. Venter, J. J., and Vannice, M. A., *Appl. Spectrosc.* **42**, 1096 (1988).
20. Delgass, W. N., Haller, G. L., Kellerman, R., and Lunsford, J. H., "Spectroscopy in Heterogeneous Catalysis." Academic Press, New York, 1979.
21. Jehng, J. M., *J. Phys. Chem. B* **104**, 462 (1998).
22. Vuurman, M., Wachs, I. E., and Hirt, A. M., *J. Phys. Chem.* **95**, 9928 (1991).
23. Deo, G., Eckert, H., and Wachs, I. E., *Prep. Am. Chem. Soc. Div. Petrol. Chem.* **35**(1), 16 (1990).
24. Went, G. T., Oyama, S. T., and Bell, A. T., *J. Phys. Chem.* **94**, 4240 (1990).
25. Oyama, S. T., Went, G. T., Lewis, K. B., Bell, A. T., and Somorjai, G., *J. Phys. Chem.* **93**, 6786 (1989).
26. Reddy, B. M., Narsimha, K., Sivaraj, C., and Rao, P., *Appl. Catal.* **55**, 11 (1989).
27. Cristinai, C., Forzatti, P., and Busca, G., *J. Catal.* **116**, 586 (1989).
28. Wachs, I. E., Jehng, J. M., Deo, G., Weckhuysen, B. M., Guliants, V. V., and Benziger, J. B., *Catal. Today* **32**, 47 (1996).
29. Wachs, I. E., and Weckhuysen, B. M., *Appl. Catal. A* **157**, 67 (1997).
30. Burcham, L., Deo, G., Gao, X., and Wachs, I. E., *Topic in Catalysis* **11/12**, 85 (2000).
31. Xie, S., Iglesia, E., and Bell, A. T., *Langmuir* **18**, 7162 (2000).
32. Yamagushi, T., Nakano, Y., and Tanabe, K., *Bull. Chem. Soc. Jpn.* **51**, 2482 (1978).
33. Davydov, A. A., *Kinet. Catal.* **38**, 836 (1997).
34. Bettahar, M. M., Costentin, G., Savary, G., and Lavalley, J. C., *Appl. Catal. A* **145**, 1 (1996).
35. Zhao, Z., and Wachs, I. E., *Division of Surface Characterization of Heterogeneous Catalysts for Partial and Complete Oxidation Reactions,* ACS presentation (paper No. 212), Chicago Meeting, Aug. 26–30, 2001.
36. Watling, T. C., Deo, G., Seshan, K., Wachs, I. E., and Lercher, J. A., *Catal. Today* **28**, 139 (1996).
37. Iglesia, E., Bell, A. T., and Wachs, I. E., private communication.
38. Adamski, A., Sojka, Z., Dyrek, K., Che, M., Wendt, G., and Albrecht, S., *Langmuir* **15**, 5733 (1999).